MAGNETIC PROPERTIES OF FERROMAGNETIC STEELS UNDER DIFFERENT STRESS BY THE ALTERNATING CURRENT MAGNETIZATION

by

Ming WEI[a,b], Zhan-Guo MA[a], Dao-Xiang TENG[b], Qing CHEN[b], Qiang LIU[b,d], Chun-Hao YIN[c*], and Zhen-Kun XU[c]

[a] State Key Laboratory for GeoMechanics and Deep Underground Engineering, China University of Mining and Technology, Xuzhou, China
[b] School of Mathematics and Physics, Xuzhou University of Technology, Xuzhou, China
[c] School of Physics, China University of Mining and Technology, Xuzhou, China
[d] School of Mechatronic Engineering, China University of Mining and Technology, Xuzhou, China

Original scientific paper
https://doi.org/10.2298/TSCI180820212W

The alternating current magnetic characteristics of the ferromagnetic materials act a significant factor to reflect their stress states. To reveal the relationship between the stress and the magnetic properties of the ferrimagnetic steels, we deduce the relation of alternating current permeability and the detected voltage of the nine-feet probe by using the basic laws in magnetism and law of electromagnetic reaction, and then we use the nine-feet probe to design and build the electromagnetic measurement system. Next some corresponding experiments were carried out to test the induction voltage of the two kinds Q-steel samples under the different stress. The results were shown that there was a similar variation tendency of the detected voltage in the two kinds the Q-steel samples, the max different values of the detected voltage can be reach 150 mV in the Q215 sample and 280 mV in the Q275 sample, respectively. Therefore, with the help of the difference detected voltage we can check the stress state of the ferrimagnetic steels conveniently in the engineering.

Key words: *ferromagnetic materials, magneto-mechanical characterizer, alternating current permeability*

Introduction

Ferromagnetic materials are widely used in the electric power, railway, pressure vessels, and other industries. In the use of materials, the stress concentration and fatigue would cause safety accidents if not be found and dealt with in time. Therefore, it is of great significance to detect the stress concentration and fatigue quickly and accurately.

In the magnetic detection, the permeability is one of the most important parameters of the ferromagnetic materials, which can reflect the information of the stress [1], fatigue [2], physical and chemical properties [3]. At present, the most frequently used methods to obtain the magnetic characteristics of the ferromagnetic materials are the direct current (DC) magnetization and hysteresis loop [4]. However, in the DC magnetic processing, there is a requirement of large coil and current to saturate the materials, which is inconvenient to the on-line detection.

* Corresponding author, e-mail: chunhaoyin@163.com

Compared with the DC magnetization, the alternating current (AC) magnetization can make materials saturated only with the small current and coil, which is convenient for the on-line measurement.

The AC magnetization method was first proposed by Katragadda and his collaborators to the detection of surface cracks in the ferromagnetic materials [5], Gotoh [6] used the AC magnetization method to establish the crack analysis model using the finite element methods. Guo [7] and Kang [8] analyzed the signals on the surface of the X80 steel pipes. Yin [9, 10] tested the residual stress distribution of the steel plate by four-feet probe, and the results showed a good agreement with the stress-strain methods. In the 2017, the magnetic signals of the surface and internal crack of the thick steel plates were studied by Tsukada, *et al*. [11].

In this paper, we use the basic laws in magnetism and Faraday's law to deduce the relation between the permeability and the detected voltage under the conditions of the AC magnetization, and in the meanwhile, we also design and build an experimental system. Based on the system, some corresponding tests were carried out by using the nine-feet probe and the results were analyzed too.

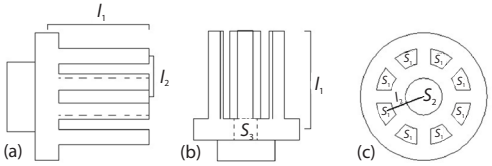

Figure 1. The structure of the nine-feet probe; (a) the side view, (b) the side view, and (c) the top view

The permeability derivation of nine-feet probe

The structure of the nine-feet probe is shown in fig. 1 [11, 12], the middle foot is the detection coil, the S_2 is its sectional area. The others feet are excitation coils and the S_1 are their sectional area. When the AC current was loaded on the excitation coils, an altering flux Φ_m will be generated, then the Φ_m can form a closed magnetic circle among the excitation coil, detection coil and the tested sample, see the fig. 2. According to the theory of magnetic circuit [13, 14] and Kirchhoff's law of magnetic circuit [15, 16], the magnetic motive force, F_m, can be written:

$$F_m = n_1 i = \sum_i H_i l_i \tag{1}$$

where n_1 is the turns of the excitation coil, i – the current of the excitation, H_i – the magnetic field intensity, and l_i – the magnetic path length.

By considering relation between the magnetic field intensity H_i and the magnetic induction intensity B_i, we can get the next equation:

$$B_i = \mu_i H_i, \; B_i = \frac{\Phi_m}{S_i} \tag{2}$$

where μ_i is the permeability, S_i – the cross-sectional area, and Φ_m – the magnetic flux.

Submitting the eq. (2) into eq. (1), eq. (3) can be obtained:

$$F_m = n_1 i = \Phi_m \sum_i \frac{l_i}{\mu_i S_i} \tag{3}$$

In the nine-feet probe, there are eight excitation feet and one detection feet. Each the excitation foot and the detection foot can form a closed magnetic circle. Therefore, the full magnetic flux of the detection foot Φ_f can be written:

$$\Phi_f = 8\Phi_m = \frac{8 n_1 i}{\sum_i \frac{l_i}{\mu_i S_i}} \tag{4}$$

Making use of the Faraday's law [17], the electromotive force $\varepsilon(t)$ of the detection foot can be written:

$$\varepsilon(t) = -n_2 \frac{\mathrm{d}\Phi_f}{\mathrm{d}t} = -\frac{8n_1 n_2}{\sum_i \frac{l_i}{\mu_i S_i}} \frac{\mathrm{d}i}{\mathrm{d}t} \tag{5}$$

where n_2 is the turns of the detection coil, i – the current of the excitation coils, expressed by $i = A\sin\omega t$, ω – the angular frequency, and A – the current amplitude. Submitting i into eq. (5), we can get:

$$\varepsilon(t) = -n_2 \frac{\mathrm{d}\Phi_f}{\mathrm{d}t} = \frac{8n_1 n_2}{\sum_i \frac{l_i}{\mu_i S_i}} \frac{\mathrm{d}i}{\mathrm{d}t} = -\frac{8n_1 n_2}{\sum_i \frac{l_i}{\mu_i S_i}} A\omega \cos\omega t \tag{6}$$

By acting the integral RC on eq. (6), the detection voltage $U(t)$ can be written:

$$U(t) = -\frac{1}{RC}\int \varepsilon(t)\mathrm{d}t \tag{7}$$

where R and C are the resistance and the capacitance of the integrator, respectively. With the aid of the experimental data [18], we have:

$$\frac{U_{\mathrm{eff}}}{\varepsilon_{\mathrm{eff}}} = \frac{1}{2fRC}\alpha \tag{8}$$

where U_{eff} and ε_{eff} are the effective values of $U(t)$ and $\varepsilon(t)$, respectively, f – the frequency, and α – the dimensionless parameter, which is related of the frequency f.

By combining eqs. (7)-(9), the relationship between the U_{eff} and the permeability can be expressed:

$$U_{\mathrm{eff}} = 5.656\frac{\alpha n_1 n_2}{\pi fRC}\frac{A\omega}{\sum_i \frac{l_i}{\mu_i S_i}} \tag{9}$$

Based on the basic laws in the magnetism [17], the sum reluctance of each magnetic path, fig. 2, can be expressed:

$$\sum_i \frac{l_i}{\mu_i S_i} = \frac{l_1}{\mu_0 \mu_{r-t} S_1} + \frac{l_1}{\mu_0 \mu_{r-t} S_2} + \frac{l_2}{\mu_0 \mu_{r-t} S_3} + \frac{l_2}{\mu_0 \mu_{r-s} S_4} \tag{10}$$

where S_1 is the cross-section of each excitation feet, S_2 – the cross-section of detection feet, S_3 – the cross-section area of probe base, S_4 – the cross-section of sample, l_1 – the length of the each foot, l_2 – the distance between the foot and the ones around it, see fig. 2, μ_0 – the permeability of the vacuum, μ_{r-t} – the relative permeability of nine-feet probe, and μ_{r-s} – the relative permeability of sample.

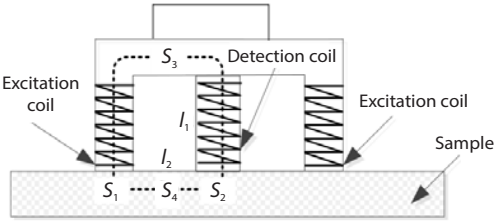

Figure 2. Measurement schematic diagram of experimental sample

Submit the eq. (10) into the eq. (9), the relation of the detection voltage U_{eff}, the relative permeability of the nine-feet probe μ_{r-t} and the sample μ_{r-s} can be written:

$$\frac{l_1}{\mu_0 \mu_{r-t} S_1} + \frac{l_1}{\mu_0 \mu_{r-t} S_2} + \frac{l_2}{\mu_0 \mu_{r-t} S_3} + \frac{l_2}{\mu_0 \mu_{r-s} S_4} = \frac{0.707}{\pi fRC} 8\omega n_1 n_2 \frac{A}{U_{s-\mathrm{eff}}}\alpha \tag{11}$$

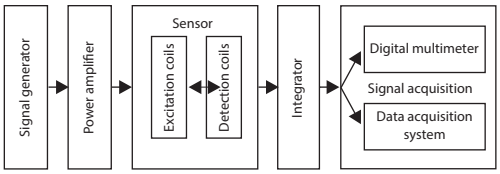

Figure 3. The measurement system

Ferromagnetic measurement experiment system

In this section, the experimental system of the AC magnetization is designed and constructed to test the relationship between the permeability and stress of the samples under the conditions of the alternating magnetization [18-21], as shown in fig. 3.

Here the signal generator can generate the several different AC signals such as the sine wave, square wave, triangle wave, and so on. In the processing of the test, the sine wave is adopted as signal source whose amplitude and frequency are adjustable. By the power amplifier, the signal from the generator can be transformed to more stable and higher-power sinusoidal signal, which is loaded into the excitation coil to generate a stable excitation magnetic field. If the detection coil is used to receive the changes of magnetic flux and output voltages, then the voltage can be detected by the digital multimeter (or data acquisition system) after the integrator amplified, as shown in fig. 3.

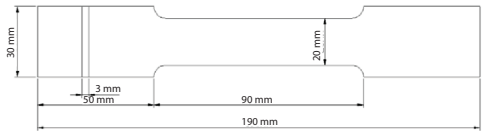

Figure 4. Illustration of the samples structure

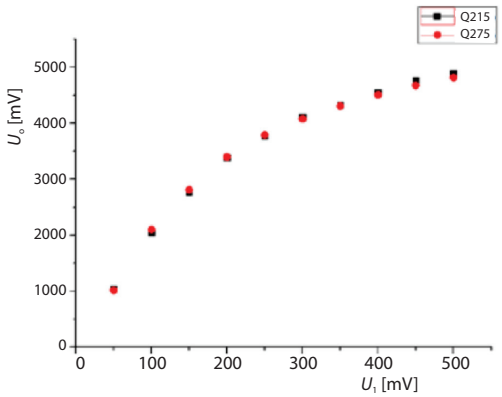

Figure 5. The relationship curve between U_0 and U_1 of the samples under the conditions of the F_s = 0 kN

In this experiment, two different kinds of the Q-steels were tested under the conditions of the static load. The sizes of the samples are showed in fig. 4. The testing results shows that the yield strengths of the Q-steel samples are about 235 MPa. With the use of records the tests are carried out under the conditions of the stress force, F_s, steps every 3 kN for the samples.

In the test, the samples were the subjected to static load and the detected probe was placed in the center of the specimens. When F_s = 0 kN, the relationship of the permeability detected voltage, U_0, and the excitation voltage, U_1, of the two samples are plotted in fig. 5. When the values of U_1 changing from 0-200 mV, U_0 of two samples approximately linearly increase and they are nearly equal. When the values of U_1 are larger than 200 mV, U_0 of two samples slowly increase and tend to stability. There is a little difference that, when U_1 is greater than 200 mV, U_0 of Q215 is larger than that of Q275.

The relation curve of the AC permeability detected voltage difference ΔU_0 and the U_1 of two samples under the different conditions of the F_s are showed in fig. 6. Here the curve of ΔU_0 of two kinds of Q-steel samples are similar to the U_0 under the conditions of F_s = 0 kN. When U_1 can be written as 500 mV and 400 mV, the maximum values of ΔU_0 are 300 mV and 140 mV for Q215 and Q275 (at F_s = 18 kN), respectively.

From figs. 5 and 6, it is illustrated that, when the U_1 is smaller than 150 mV, the ΔU_0 decreases with the increase of F_s. Since the bounded of the movement of magnetic domain toward external magnetic field, it leads to the reduce of the magnetizations of the samples. When the U_1 is larger than 150 mV under the stress and external magnetic field, the magnetic switching effect appears in the process of sample magnetization [22-26].

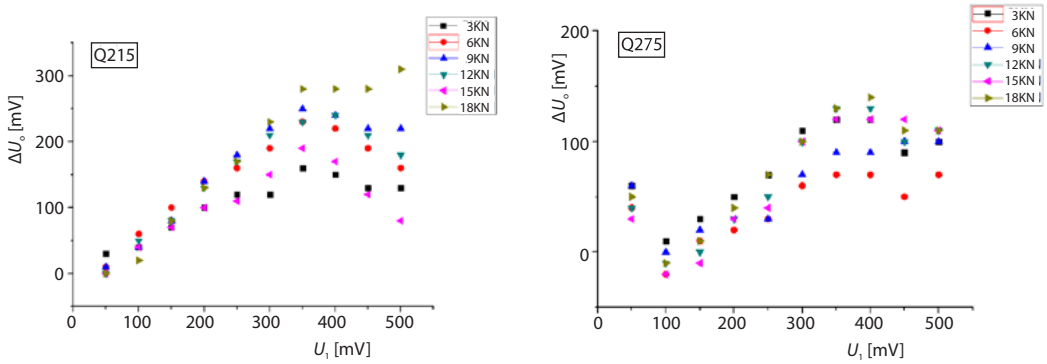

Figure 6. The relation curve between ΔU_0 and U_1 of two samples under the conditions of the F_s at different values; (a) the sample of Q215, (b) the sample of Q275

Due to the changes of the permeability, the exciting voltage and F_s can be discussed as follows. On one hand, the different F_s can lead to the different levels of the magneto strictive effects, and the changes of the AC permeability of the samples. On the other hand, there is a tendency in the samples to dislocate under the conditions of the stress when the dislocation happens. When it makes the materials hander, it results in the reduction of the mobility of the dislocation. Moreover, the dislocation slip of the crystal in the samples leads to the great difference of the magnetic properties, when the reversal effect of the magnetization would occur in the samples.

Conclusion

In our work, we deduced therelationship between the detection voltage and the relative permeability of the samples by using the Faraday's law and the basic magnetism laws. We also constructed the AC magnetic detection system with the nine-feet probe,then two different kinds of Q-steels were tested by this system. It is showed that there is a significant difference in detection voltage values of the relative permeability of the samples under different stress conditions, F_s, the maximum values ΔU_0 can reach 300 mV.

Acknowledgment

The work is supported by the Key Program of the National Natural Science Foundation of China (Grant No. 50834005), the National Key R and D Program of China (Grant No. 2017YFC0804401),the National Natural Science Foundation of China (Grant No. 51674250), the Fundamental Research Funds for the Central Universities (No. 2010QNB25 and 2012LWB66), the Natural Science Foundation of Jiangsu Province (No. BK2009092).

Nomenclature

A – current amplitude, [A]
B – magnetic introduction intensity, [T]
C – capacitance, [F]
f – frequency, [Hz]
F_m – magnetic motive force, [A]
F_s – stress force, [kN]
H – magnetic field strength, [Am^{-1}]
i – AC current, [A]
l – length, [m]
n – coil winds
n_1 – turns of the excitation coil, [–]
n_2 – turns of the detection coil, [–]
R – resistance, [Ω]
S – cross-sectional area, [m^2]
S_1 – cross sectional area of one excitation coil, [m^2]
S_2 – cross sectional area of one detection coil, [m^2]
S_3 – cross sectional area of the probe base, [m^2]
S_4 – cross sectional area of the simple, [m^2]

t – time, [s]
U – voltage, [V]
U_0 – permeability detected voltage, [mV]
ΔU_0 – permeability detected voltage difference, [mV]
U_1 – the excitation voltage, [mV]
$U(t)$ – voltage, [V]
U_{eff} – effect value of $U(t)$, [V]
$U_{s\text{-eff}}$ – detection voltage effect value of the sample, [V]

Greek symbols

α – dimensionaless parametar
$\varepsilon(t)$ – electromotive force, [V]
ε_{eff} – effect value of $\varepsilon(t)$,[V]
μ – magnetization permeability, [Hm^{-1}]
μ_0 – permeability of the vacuum, [Hm^{-1}]
$\mu_{R\text{-}t}$ – relative permeability of nine-feet probe
$\mu_{R\text{-}s}$ – relative permeability of sample
Φ – magnetic flux, [Wb]
Φ_f – full magnetic flux of the detection coil, [Wb]
Φ_m – magnetic flux between one excitation coil and the detection coil, [Wb]
ω – angular frequency, [rads $^{-1}$]

Reference

[1] Xing, L., *et al.*, Review on the Steel Magnetic Permeability Detection Method (in Chinese), *Physical Experiment of College*, *26* (2013), 6, pp. 31-35
[2] Qiu, Y., *et al.*, Research on Magnetic Signals on Surface of Ferromagnetic Specimen after Tension Fatigue under Weak Magnetic Field (in Chinese), *New Technology and New Process, 34* (2013), 5, pp. 66-69
[3] Liu, H.-S., *et al.*, Theoretical Analysis of Magnetic Sensor Output Voltage, *Journal of Magnetism and Magnetic Materials, 323* (2011), 12, pp. 1667-1670
[4] Li, L-M., *et al.*, The AC and DC Magnetizing for Magnetic Flux Leakage Testing (in Chinese), *Journal of Tsinghua University (Scinece and Technology) , 42* (2002), 2, pp. 154-156
[5] Katragadda, G., *et. al*., Alternative Magnetic Flux Leakage Modalities for Pipe-Line Inspection, *IEEE Transactions on Magnetics, 32* (1996), 3, pp. 1581-1584
[6] Gotoh, Y., *et al.*, The 3-D Non-Linear Eddy-Current Analysis of Alternating Magnetic Flux Leakage Testing-analysis of One Crack and Two Cracks, *IEEE Transactions on Magnetics, 38* (2002), 2, pp. 1209-1212
[7] Guo, X.-L., *et al.*, Application of Alternative Current Magnetic Leakage Flux Method for Surface Defect Recognition of Steel Pipe (in Chinese), *Sensor World, 11* (2005), 7, pp .6-8
[8] Kang, Z.-W.,, *et al.*, Alternative Magnetic Flux Leakage Testing System for Detecting Surface Defect of Steel Pipe (in Chinese), *Non-Destructive Testing, 28* (2006), 4, pp. 189-191
[9] Yin, C.-H., *et al.*, A Magnetically Anisotropy Method for Measuring Residual Stress in the Steels (in Chinese), *Journal of Test and Measurement Technology, 21* (2007), 1, pp. 28-32
[10] Yin, C.-H., *et al.*, Influence of the Condition of Magnetism Stress Measurement on the Stress Sensitivity (in Chinese), *Journal of Test and Measurement Technology, 20* (2006), 1, pp. 11-14
[11] Tsukada, K., *et al.*, Detection of Inner Cracks in Thick Steel Plates Using Unsaturated AC Magnetic Flux Leakage Testing with a Magnetic Resistance Gradiometer, *IEEE Transactions on Magnetics, 53* (2017), 11, 2501305
[12] Gong, J.-H., *et al.*, A New Method for Calibrating the Sensitivity Coefficient of Magnetic Residual Stress Meter (in Chinese), *Measurement Technique, 2* (2015), pp. 23-26
[13] Zhao, Y., *et al.*, Maxwell's Equations on Cantor Sets: A Local Fractional Approach (in Chinese), *Advanced in High Energy Physics*, *2013* (2013), ID 686371
[14] Yang, X. J., *et al.*, Srivastava, *Local Fractional Integral Transforms and Their Applications*, Academic Press, Elsevier, Amsterdam, The Netherland, 2015
[15] Yang, X. J., *et al.*, On a Fractal LC-Electric Circuit Modeled by Local Fractional Calculus, *Communications in Non-linear Science and Numerical Simulation, 47* (2017), June, pp. 200-206
[16] Sudhoff, S. D., *Power Magnetic Devices: A Multi-Objective Design Approach*, Wiley-IEEE Press, New York, USA, 2014
[17] Carson, J. R., *et al.*, Electromagnetic Theory and the Foundations of Electric Circuit Theory, *Bell System Technical Journal, 6* (1927), 1, pp. 1-17
[18] Xu, Z.-K., Basic Research of Measurement Methods of Magnetism of Materials (in Chinese), M. Sc. thesis, Xuzhou: China University of Mining and Technology, 2014, pp. 17-18
[19] Zhau, Z., *et al.*, Design of Plane Welding Residual Stress Sensor with Nine Magnetic Pole (in Chinese), *Instrument Technique and Sensor*, (2012), 6, pp. 8-10
[20] Deng, D.-G., *et al.*, Measurement of Initial Magnetization Curve Based on Constant Magnetic Field Ex-cited by Permanent Magnet (in Chinese), *Acta PhysicaSinica, 65* (2016), 14, pp. 8101-8109

[21] Deng, D.-G., *et al.*, A Method of Characterizing Axial Stress in Ferromagnetic Members Using Superficial Magnetic Flux Density Obtained from Static Magnetization by Permanent Magnet (in Chinese), *Acta PhysicaSinica, 67* (2018), 17, pp. 331-342
[22] Ren, S.-K., *et al.*, Magnetizing Reversion Effect of Ferromagnetic Specimens in Process of Stress-Magnetizing (in Chinese), *Journal of Iron and Steel Research, 22* (2010), 12, pp.48-52
[23] Fan, Z., *et al.*, Influences of the Demagnetizing Field on Dynamic Behaviors of the Magnetic Domain Wall in Ferromagnetic Nanowires (in Chinese), *Acta PhysicaSinica, 61* (2012), 10, pp. 398-404
[24] Zhang, N., *et al.*, Progress of Electrical Control Magnetization Reversal and Domain Wall Motion (in Chinese), *Acta PhysicaSinica, 66* (2017), 2, pp. 1-10
[25] Shi, P.-A., *et al.*, Study on the MicroMechanical Model of Force-magnetic Coupling for Ferrogel Materials (in Chinese), *Journal of Mechanical Strength, 39* (2017), 3, pp.564-571
[26] Zu, R.-L., *et al.*, Study on the Influence of Magnetic Field on Force-magnetic Coupling Relationship of Ferromagnetic Specimen (in Chinese), *China Measurement and Test, 43* (2017), 10, pp. 123-133

Paper submitted: August 20, 2018
Paper revised: November15, 2018
Paper accepted: January 13, 2019